Brazilian Maize Yields Negatively Affected By Land Clearing

Stephanie A. Spera[1,2,3], Jonathan M. Winter[3,4], Trevor F. Partridge[4]

[1] Department of Geography and Environment, University of Richmond, Richmond, VA, USA
[2] Neukom Institute for Computational Science, Dartmouth College, Hanover, NH USA
[3] Department of Geography, Dartmouth College, Hanover, NH, USA
[4] Department of Earth Sciences, Dartmouth College, Hanover, NH, USA

Abstract

To date, over 50% of the Brazilian Cerrado has been cleared predominantly for agropastoral purposes. Here, we use the Weather Research and Forecasting model to run 15-year climate simulations across Brazil with six land-cover scenarios: 1) before extensive land clearing; 2) observed in 2016; 3) Cerrado replaced with single-cropped (soy) agriculture; 4) Cerrado replaced with double-cropped (soy-maize) agriculture; 5) eastern Amazon replaced with single-cropped agriculture; and 6) eastern Amazon replaced with double-cropped agriculture. All land-clearing scenarios (2-6) contain significantly more growing season days with temperatures that exceed critical temperature thresholds for maize. Evaporative fraction significantly decreases across all land-clearing scenarios. Altered weather reduces maize yields between 6–8%, when compared to the before extensive land clearing scenario; however, soy yields were not significantly affected. Our findings provide evidence that land clearing has degraded weather in the Brazilian Cerrado, undermining one of the main reasons for land clearing: rainfed crop production.

Main

Deforestation and land clearing for agropastoral purposes in Brazil have been linked to myriad negative environmental consequences, such as decreases in biodiversity[1–3], evapotranspiration rates[4–6], and carbon storage [7], and increases in temperature[8,9], dry season length[10–13], streamflow[14–16], fire occurrence[17], and CO_2 emissions[18–20]. However, crop and livestock production are essential to Brazil's economy. In 2018, agribusiness alone generated more than a fifth of Brazil's total GDP and Brazil is ranked in the top three for global soy and maize production and exports[21]. In 2019, maize production increased by 18% due to both cropland expansion and a productive "safrinha" (second crop in a double-cropped rotation) season[22].

Brazil's rise to becoming a major global breadbasket has come most recently at the expense of the Cerrado and southeastern Amazon (white box, Figure 1a), the focus of this paper. In this region, only 6% of cropland is irrigated[23]; and a majority of the fields are double-cropped, often first planted with a soy "safra" rotation, followed by a second, maize "safrinha" ('*little harvest*') rotation. Farmers here depend on a predictable and stable rainy season to successfully cultivate export agriculture, however, the modern heavily fragmented landscapes have created edge effects with varying impacts on precipitation[24–26], likely through altered convection[27]. And Amazon-focused studies have shown that the expansion of agriculture could create a 'no-win scenario'[28], where agricultural productivity decreases as agricultural land increases due to the effects of land-cover conversion on regional climate[4,28,29]. Understanding how land-cover changes affect regional climate in the Brazilian Cerrado is critically important for maximizing food production while minimizing environmental damage.

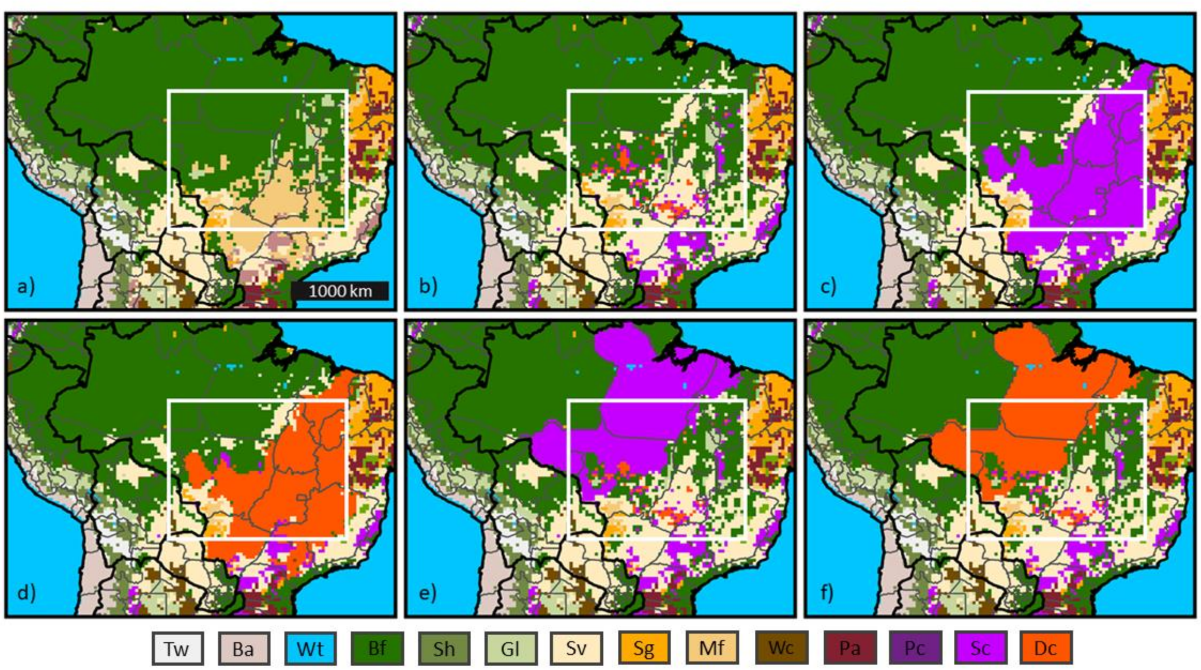

Figure 1. WRF model run domain and the six land cover scenarios. a) Brazil before land clearing (BzBLC), white box indicates our region of interest and the focus of our statistical analyses; b) Brazil 2016 (BZ16); c) Cerrado single-cropped (CeSC); d) Cerrado double-cropped (CeDC); e) Amazonian deforestation arc states (Tocantins, Pará, Mato Grosso, and Rodônia) single-cropped (AzSC); and f) Amazonian deforestation arc states double-cropped (AzDC). Legend key: Tw = wooded tundra; Ba = barren/sparsely vegetated; Wt = water; Bf = evergreen broadleaf forest; Sh = shrubland; Gl = grassland; Sv = savanna; Sg = mixed shrubland/grassland; Mf = mixed forest; Wc = woodland/cropland mosaic; Pa = pasture; Pc = mixed cropland/pasture; Sc = single cropped agriculture; Dc = double cropped agriculture.

Climate modelling studies generally support observations, demonstrating that tropical deforestation increases local temperatures[9,30] and Amazonian deforestation exacerbates drought conditions and increases the length of the dry season in the southeastern Amazon[31–33], consequently escalating fire risk[34]. Highly fragmented landscapes with small-scale vegetation may enhance rainfall through the convection triggered as a result of greater sensible to latent heat ratios[35], but at regional and global scales, critical thresholds exist where tropical deforestation could lead to significant decreases in precipitation because less water is recycled back through the atmosphere[30]. The Cerrado plays an integral role in supporting stable rainfall over the Amazon, as air masses traveling over the Cerrado to the Amazon gain additional moisture from the evapotranspiration of Cerrado vegetation[29,36]. Lastly, the land cover that replaces cleared areas matters: replacing all deforested areas in the Amazon with soybean may lead to greater decreases in precipitation than replacing them with pasture grasses because of differences in albedo and evaporatranpiration[37].

Examining the interactions between intensive double-cropping and land-use change in Brazil is critical for multiple reasons: 1) double-cropping rotations comprise a majority of agriculture across the southeastern Amazon and Cerrado; 2) studies have demonstrated that compared to single-cropping, double-cropping rotations transpire similar amounts of water to the atmosphere as native Cerrado vegetation for a greater portion of the year[5]; and 3) the ability to double-crop is contingent on a climatologically predictable growing season[38]. Here, we examine these interactions by running six 15-year (2000-2015) simulations of the National Center for Atmospheric Research's Advanced Research Weather Research and Forecasting Model (WRF) with six different land-use scenarios (Figure 1): 1) Brazil before land clearing (BzBLC); 2) Brazil 2016 (Bz2016); 3) Cerrado in single cropping (CeSC); 4) Cerrado in double cropping (CeDC); 5) Amazon deforestation arc in single cropping (AzSC); and 6) Amazon deforestation arc in double cropping (AzDC). WRF generally reproduces precipitation in this region; however, the model underestimates temperature (a ~2°C cold bias) during the rainy season (Nov – Apr), and overestimates evapotranspiration (~200 mm/year) with the largest biases occurring during the early wet-season (Sept-Dec) (see Methods, SI, and Spera et al.[39] for more details).

We quantify the effects of historical and potential land-use change on the regional climate along the Brazilian Cerrado-Amazon border, a region that has experienced much of the land-clearing and expansion of intensive export agriculture since the mid-1990s (Figure 1) and is crucial for regional climate regulation[1]. We then assess the implications of these changes on the production of soy (Sept 15 – Jun 15 growing season) and maize (Jan 15 – Aug 15 growing season). This study importantly highlights the tradeoffs between conservation, crop-management, and sustainable agricultural development.

Evaporative Fraction and Temperature Differences are Largest in the Wet-Dry Season Transition

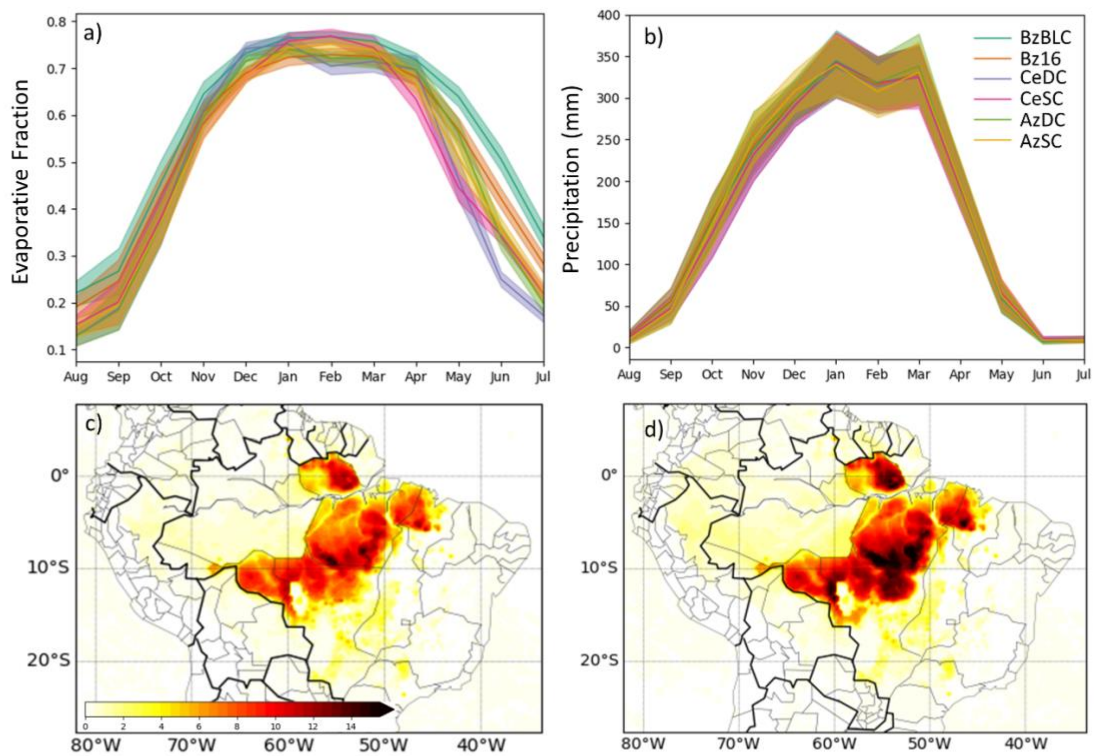

Figure 2. Seasonal cycles of a) evaporative fraction and b) precipitation spatially averaged across our region of interest (white box in Figure 1a). The solid lines represent mean monthly values, and the shaded area represents bootstrapped 95% confidence intervals. Results for minimum and maximum temperature, and subregions are presented in the supplementary information. Average increase in the number of maize warm nights (> 24°C) over the maize growing season (Jan – Aug) for the c) AzDC scenarios and d) AzSC scenario as compared to the BzBLC scenario.

There are significant differences (significance, here and throughout, is defined as non-overlapping bootstrapped 95% confidence intervals) between some scenarios and BzBLC in evaporative fraction—the ratio of latent heat to total available energy at surface, minimum temperature, and maximum temperature during the dry season (June-August), and the wet/dry (September) and dry/wet (April-May) season transition months (Figure 2, SFigure 3). The monthly evaporative fraction is significantly higher in the BzBLC scenario than all other scenarios during the months of May, June, and July (Figure 2a). During August, the evaporative fraction of all but the Bz16 scenario is significantly lower than the BzBLC (Figure 2a). The BzBLC scenario has cooler minimum and maximum temperatures in all months except December, January, February and March (SFigure 3). This feature is likely a result of managed crops transpiring at similar rates as Cerrado vegetation during the months of December, January, February, and March—the height of the agricultural growing season[5]. Evaporative fraction over double-cropped agricultural areas is closer to evaporative fraction over native Cerrado vegetation from January through April, and temperature increases are greater under the single cropping scenarios (Fig 2d) than the double-cropping scenarios (Fig 2c), providing further evidence of the similarities in latent and sensible heat energy partitioning between Cerrado vegetation and double-cropped fields.

Evapotranspiration rates are significantly reduced

Annual evapotranspiration is significantly reduced across all scenarios when compared to BzBLC (SFigure 4a): the mean decrease in annual evapotranspiration between BzBLC and Bz16 is over 6% and between BzBLC and the Cerrado and Amazon clearing scenarios is over 14%. Dry-to-wet transition season (SON) evapotranspiration is reduced across all scenarios and significantly reduced across all but the Bz16 scenario (SFigure 4b). During the dry-season and dry/wet season transition months, we find similar available energy, but more sensible heat because of the reduction in transpiration due to land clearing. This change in energy partitioning is crucial because dry season transpiration is key to initiating the rainy season. These results agree with previously published work demonstrating the direct effects of large-scale land-clearing for export agriculture[5,15,16].

Exceedances of critical minimum and maximum temperature thresholds increase

During the soy growing season (September – June) all but the Bz16 scenario result in significantly more days with a maximum temperature above 40°C (hereafter "soy hot days") when compared to the BzBLC scenario (Figure 3a). The Cerrado conversion scenarios (CeSC and CeDC) result in five more soy hot days per season, and the southeastern Amazon conversion scenarios (AzSC and AzDC) result in an average increase of over seven soy hot days per season. These additional hot-days occur early in the growing season, September–November (SFig 7), coincident with decreased evapotranspiration (Fig 2a).

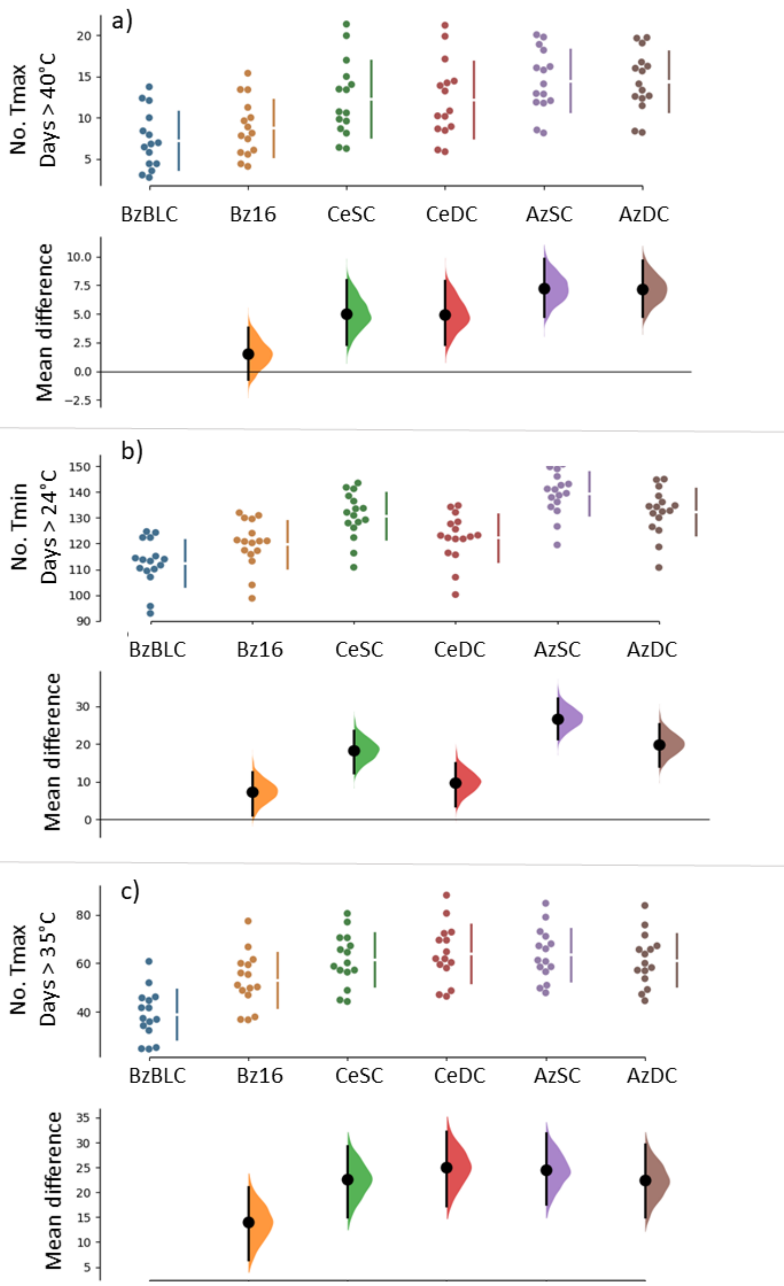

Figure 3. Estimation plots of a) the number of days in the soy growing season with a maximum temperature above 40°C, b) the number of days in the maize growing season with a minimum temperature above 24°C, and c) the number of days in the maize growing season with a maximum temperature above 35°C. Each point in the scatter plot represents the spatial average over the whole region of interest for the 15 (2001 – 2015) harvest years (top), with bootstrapped 95% confidence intervals of the effect size (bottom).

All five scenarios also have significantly more nights with a minimum temperature above 24°C (hereafter "maize warm nights") than the BzBLC scenario (Figure 3b), again coincident with decreased evapotranspiration. The Bz16 scenario has the smallest increase in warm nights (8 per season) (Figures 3b). The mean maize warm nights increase in the CeSC, AzSC, and AzDC scenarios relative to the BzBLC scenario ranges from 20 – 30 warm nights per season, with the Amazon-clearing scenarios resulting in the largest increases in warm nights (Figure 2c,d Figure 3b). Double-cropping scenarios have fewer maize warm nights than the single-cropping scenarios because the presence of *safrinha* maize decreases minimum temperatures Mar-Jun through prolonged and increased evapotranspiration (SFigures 3, 8, 10). Besides evapotranspiration, no other temperature-independent variable seemed to mimic the signal that is the increase in minimum temperatures. Increases in minimum temperatures are most pronounced in the Mato Grosso region (Figure 2c,d, SFigure 19), where over 30,000 tons of *safrinha* maize (42% of the Brazil's *safrinha* maize) was harvested in 2019[40].

During the maize growing season (January – August), all five scenarios also have significantly more days with maximum temperature above 35°C (hereafter "maize hot days") than the BzBLC scenario (Figure 3c). Again, the Bz16—the scenario with the least amount of natural vegetation converted to cropland—has the smallest increase in maize hot days. As with soy hot days, the increase in maize hot days is coincident with reduced evapotranspiration over the growing season (SFigure 10). Unlike with maize warm nights, the number of maize hot days is not affected by whether the scenario is single or double cropped because a large number of hot days occur in June and July (SFigure 9), where differences in evapotranspiration among the scenarios is muted.

Precipitation does not significantly decrease

We focused our analysis on annual precipitation, seasonal precipitation, and precipitation at the start of the rainy season (September-October) as previous studies have demonstrated that farmers decide whether or not to double-crop during these two months[38]. Averaged across the whole region of interest, annual precipitation, start of the rainy season date, end of rainy season date, and precipitation during the start of the rainy season (September-October) did not decrease or change significantly for any scenario (SFigure 5, SFigure 6, SFigure 11a). However, precipitation during the start of the rainy season (September-October) did significantly decrease in the Tocantins sub-region between BzBLC and both Amazon clearing scenarios (SFigure 11b). The delayed start of the rainy season in this region may be linked to a large but insignificant decrease in June, July, August precipitation centered over the cleared northeastern Para and northwestern Maranhão (SFigure 14), which, interestingly, is coincident with increased rain over northwestern Amazonia. This particular regional difference in the start of rainy season precipitation is notable as much of the large-scale agricultural expansion and investment in infrastructure for export agriculture over the last two decades has occurred in the Matopiba region[5,41], which is comprised of southern (Ma)ranhão, (To)cantins, southern (Pi)auí and western (Ba)hia. No other scenarios or seasons demonstrate these clear land-use associated changes in precipitation (SFigure 12, SFigure 13, SFigure 14).

As highlighted in the introduction, both observational and modelling studies have linked deforestation and agricultural expansion to decreases in precipitation and increases in dry season length across our region of interest[10,12,13,32,37,42]. We therefore expected to see a clear precipitation signal in our model output. One recent experiment with a coupled ecosystem-regional-atmospheric model demonstrated that although deforestation along the Amazon-Cerrado boundary resulted in decreases in evapotranspiration and convective available potential energy (CAPE), and increases in convective inhibition (CIN), all of which should suppress rainfall, there was no significant decrease in precipitation[43]. We suspect, then, that the lack of signal in precipitation may be due, in part, to the fact that any changes in latent heat flux, CAPE, or CIN due to land cover change are eclipsed by the larger advective patterns that create a consistently unstable atmosphere in the region[43].

Maize crop yields are reduced; soy crop yields are not affected

We quantify the potential impacts of altered weather due to each land-use scenario on maize and soy yields using a random forest algorithm trained on historical yield and climate data for the most productive microregions within the domain of interest. Forcing the crop model with climate data from the WRF simulations indicates that maize yields are reduced across all scenarios when compared to BzBLC, including Bz16. All five land-use scenarios result in a median yield decrease between 6 – 8% per year for the 36 maize microregions (Figure 4, SFigure 46). The largest yield differences are observed in the AzSC scenario where certain microregions in the Mato Grosso exhibit yield reductions of more than 20% (Figure 4), consistent with the regional differences in temperature (Figure 2c,d).

The modeled maize yield differences are driven almost entirely by differences in temperature between the WRF simulations, which is expected given the lack of precipitation change across scenarios. Accumulated local effect plots, which show the isolated effect of varying a single variable on predicted yield[44], suggest that growing season maximum temperature and the number of warm nights have the greatest influence on maize yields. Predicted partial yields decrease by ~1250 kg ha^{-1} as average growing season maximum temperature increases from 28°C to 34°C and by ~700 kg ha^{-1} as the number of maize warm nights increases from 0 nights to 50 nights (SFigure 44). Statistical crop models cannot capture the physiological mechanisms responsible for yield predictions and often underestimate the importance of precipitation[45,46]. Further work could utilize a biophysical crop model to explicitly capture the physiological mechanisms responsible for the predicted yield differences and better understand the interconnected nature of land-use, regional climate, and crop productivity in Brazil.

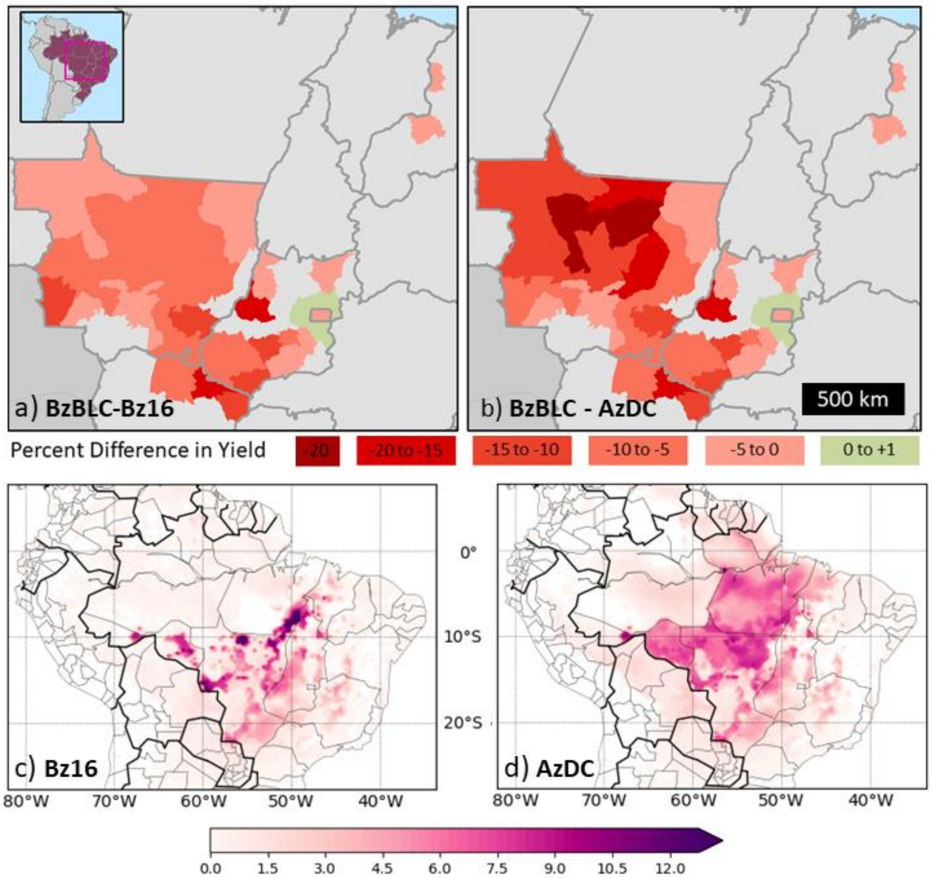

Figure 4. Percent difference in maize yields between (a) BzBLC and Bz16 and (b) BzBLC and AzDC across microregions of our study area – highlighted in the pink box in the inset. Average increase in the number of maize hot (> 35°C) days over the maize growing season (Jan – Aug) for the c) Bz16 scenarios and d) AzDC scenario as compared to the BzBLC scenario.

Modelled soy yield decreases were much smaller than maize and insignificant (SFigure 49). Accumulated local effect plots suggest that soy yields are relatively insensitive to variations in the included climate predictor variables (SFigure 47). These results are consistent with previous work, suggesting that soy is less sensitive than maize to fluctuations in temperature and precipitation[47,48].

Concluding remarks

The conversion of Cerrado and Amazon vegetation to large-scale mechanized agriculture has been essential in Brazil's ascension to a global breadbasket and crop-exporting powerhouse. Changes in temperature, runoff, fire, energy partitioning, and evapotranspiration are just some of the observable effects of these changes in land-cover and land-use. WRF is uniquely valuable for exploring the effects of land-use changes (such as converting savannah to double-cropped agriculture) and management regimes (single-cropping versus double-cropping rotations) on regional climate. However, despite the adjustments discussed in the methods and supporting information, the model continues to overestimate ground evaporation during the dry-to-wet season transition (August-October), a period that is crucial to describing land-atmosphere feedbacks in this region[11,24]. These issues with the WRF soil moisture model have been previously noted and are an obstacle to better understanding the effects of land-use change during this critical dry-to-wet season period.

This overestimation in evapotranspiration, coupled with our use of high temperature thresholds for maize and soy, means that here we present conservative results. And, our conservative results indicate that land-use changes through 2016 have significantly increased the amount of warm nights and hot days within maize and soy growing seasons, and negatively impacted maize production. Further clearing of natural vegetation for agriculture could create a regional climate that hinders the successful cultivation of temperature-sensitive export-orientated agriculture.

In the first six months of Jair Bolsanaro's presidency alone (January – June 2019) the Amazon lost 336,000 ha of forest cover – a 39% increase over the same six months in 2018 – and IBAMA (the Brazilian Institute of the Environment and Renewable Energy Resources) punitive deforestation enforcement actions decreased by 20%[49]. Given the observed impacts of land clearing, and the potential of a tipping point when modification of the landscape affects energy balances so much so that the savannization of the Amazon occurs[28–30,36,42], understanding the feedbacks between land-use change and climate is urgent.

METHODS

WRF Model

Model Set-Up

We used the National Center of Atmospheric Research (NCAR) Advanced Research Weather Research and Forecasting (WRF) model v4.0.0[50] coupled with the Noah-Mulitparameterization (Noah-MP) land-surface model[51,52]. Our model domain is 178 by 122 grid cells over northern South America, including the Cerrado and Brazilian Amazon (SFigure 1). The model was configured using a single domain at 36 km grid spacing with 120 second time step and daily output. Six-hourly European Centre for Medium Range Weather Forecast Reanalysis-Interim (ERA-I) pressure-level and surface data[53] were used as the lateral boundary conditions. We use a model configuration shown to reasonably simulate South American climate[39] (STable 1). We refer the reader to Spera et al.[39] for a complete discussion of the model bias in this region, but in short: compared to gridded CRU precipitation data, the model demonstrates a slight, but insignificant wet bias across much of the study area, similar to other studies focused on this region[54]; compared to gridded CRU temperature data, the model exhibits a cool bias across our study region that is approximately 1.6°C annually averaged, but focused during November through April (SFigure 2); and compared to MODIS evapotranspiration data[55], the model overestimates annual evapotranspiration by ~180 mm/year, with the largest overestimations occurring during September through December (SFigure 2). The model accurately simulates evapotranspiration, precipitation, and temperature May through August (SFigure 2).

Six 16-year (Jan 1, 2000 - Jan 1, 2016) simulations were conducted. January through July 2000 were used to spin-up the model, and thus our study period is defined as the 15 growing seasons beginning with the 2001 harvest year (Aug 1, 2000-July 31, 2001). These model runs output daily data. To further investigate differences in daytime and nighttime dynamics, and because certain WRF model variables are 'instantaneous' and thus our daily output values could not be used, we also ran six 6-year (Jan 1, 2010 – Jan 1, 2016) simulations that output data every three hours. Again, January through July 2010 was used to spin-up the model.

The Noah-MP land surface model (LSM)[51] allows users to choose from multiple means of combining prescribed data, such as land-cover specific average monthly leaf area index (LAI), rooting depth, vegetation fraction (FVEG), with dynamic modelling to simulate land-surface interactions. Thus, one can define vegetation parameters in three ways: 1) completely based on prescribed data from look-up tables 2) partly-based on prescribed data from look-up tables and dynamic photosynthesis-based vegetation modelling, or 3) using only the process-based photosynthesis equations from fixed land-cover categories. To date, the dynamic vegetation model both does a poor job in simulating observed Brazilian agricultural land-cover parameters such as LAI and FVEG, and cannot account for double-cropping[39]. Thus, both monthly LAI and FVEG are prescribed (STable 2) - a configuration which has been shown to accurately simulate observed land-cover and climate variables over Brazil[39].

Previous work has demonstrated that Noah-MP has difficulty in simulating soil moisture[39,56–58] and, relatedly, overestimates early wet-season ground evaporation over the Cerrado region[39]. Noah-MP is extremely sensitive to soil parameters[58]. Consistent with previous model calibrations, we multiplied the soil resistivity coefficient by twenty, and halved the soil field capacity and maximum soil water content values[51, 54] (STable 3).

The Noah-MP LSM also includes a crop model that can be turned on when dynamic vegetation is turned on. While we intend to employ this crop model in future work, at this time, it only allows for the implementation of one crop per year, and previous work has demonstrated that it does not yet accurately represent agricultural phenology in Brazil[39].

Land Cover Datasets

This study builds off work demonstrating that replacing the default WRF land cover surfaces with more accurate land cover surfaces from Spera et al.[5] improves climate model output, increasing the model performance across precipitation, evapotranspiration, and temperature variables for at least three-months, particularly during the dry-to-wet season transition, when compared to observational datasets (SFigure 2)[39]. Here, we created new land-cover maps in our region of interest for each scenario, which replaced the default WRF land-cover in those regions. Within WRF, one can choose from a USGS-based or MODIS-based land-cover. We replace the default USGS land cover map with our new land-cover map over our region of interest over the default USGS land cover because it is more accurate ensuring our region of interest has the most up-to-date accurate land-cover information[39].

The BZ16 land-cover was created following the methods of Spera et al.[39] by overlaying a MODIS Enhanced Vegetation Index-based 250 m resolution large-scale agricultural map[5] over the Landsat-based MapBiomas (v3.1) 2016 Brazilian land-cover map[59]. The BzBLC scenario was created by replacing the anthropogenic (i.e., “dryland cropland and pasture”) land cover in our study region with the nearest non-anthropogenic land-cover (e.g., “savanna”, “evergreen broadleaf forest”). In the CeSC scenario, the entire Cerrado biome was replaced with single-cropped agriculture; in the CeDC scenario, the entire Cerrado biome was replaced with double-cropped agriculture; and in the AzSC and AzDC scenarios, the Amazon-biome portion of the deforestation arc states of Rondônia, Mato Grosso, Pará, and Tocantins are replaced with single-cropped and double-cropped agriculture, respectively.

Our full model domain was comprised of 21,716 grid cells, and our region of interest (ROI, white box, Figure 1a) contained 17,768 grid cells. We chose to focus our analysis on the states of Mato Grosso, Goiás, Para, Rodônia and the Matopiba (Maranhão, Tocantins, Piauí, Bahia border) region for four main reasons: 1) because these states have been subject to a majority of the land-clearing—80% in the Amazon[60], and over 80% in the Cerrado[61,62]—and expansion of large-scale intensive export agriculture over the last two decades[63–65]; 2) these recent land-use changes have been linked to observational changes in the water and energy balance[1,10,12,13,15,16,39,66]; Brazil itself has targeted the Matopiba region to invest in its agricultural development[5,41], and most recently, soy is expanding into northern-Mato Grosso and southern Para and land-clearing rates are increasing here[67]; and 3) consistent, accurate, validated crop-specific land-cover maps are available over this region[5]. We do not include Mato Grosso do Sul, São Paulo, and Minas Gerais in our large regional analysis as much of the land in these states has been cleared for agropastoral purposes since the 1970s[68], and we do not include northern Goiás in our sub-regional analysis as much of that land has been cleared for pasture, and we were focused on the expansion of large-scale export agriculture[37]. We were interested in the effects of intensive agricultural expansion on regional climate, and thus focus on the specific sub-regions where this has occurred.

Across our ROI, average annual precipitation varies between 400 and 2,600 mm/year. Thus, we subset our ROI into four different sub-regions: 1) The Mato Grosso Amazon-Cerrado transition; 2) southwestern Mato Grosso and southern Goiás; 3) Tocantins; and 4) western Bahia, southern Maranhão, and southern Piauí (SFigure 1). However, for both brevity and clarity, a majority of the results presented in the main text have been spatially averaged across our ROI as they did not vary substantially across subregions. Results for all regions are presented in the supporting information.

Scenario Comparison

We use shared-control estimation plots to compare across scenarios, and derive 95% nonparametric bootstrap confidence intervals with 1000 resamples for each output variable of interest. These output variables are spatially averaged across each regional domain (SFigure 1), resulting in 15 data-points per region. We choose to use these estimation statistics rather than traditional significance testing (i.e., ordered group ANOVA testing) because estimation methods both focus on effect size and better facilitate data visualization than traditional box plots. To perform these analyses, we use the Data Analysis with Bootstrap Estimation v0.2.4 Python package[69]. We also compared seasonal cycles across scenarios, calculating and displaying both the mean and 95% confidence intervals.

We use published crop calendars from the Brazilian National Food Supply Company[70] to define the soy and maize growing seasons. Soy is typically the first "safra" crop, which spans September 15 - June 15. The safra crop can either be the only crop in a single-cropped rotation, or the first crop in a double-cropped rotation. In a double-cropped rotation, maize is often the second "safrinha" crop. The maize safrinha growing season spans January 15 - August 15.

We focus on minimum temperatures of 24°C for maize, and maximum temperatures of 35°C and 40°C for maize and soy, respectively, as these have been cited throughout Brazilian agronomic[71–73] and published academic[74–78] literature as the most conservative (highest) temperature limits above which production decreases. We follow the methods of Spangler et al.[38] and calculate annual accumulated precipitation anomalies to determine the start date and end date of the rainy season.

Parameterizing and Estimating Yields

We develop an empirical crop model to estimate the impact of regional climate variability on maize and soy yields using Matlab's treebagger random forest algorithm[79]. Random forest is an ensemble-based machine learning algorithm consisting of hundreds of individual regression decision trees, with each tree built with a random subsample of the observational dataset and predictor variables. Random forests have been shown to outperform simple linear regressions as they can capture the nonlinear relationships that relate plant physiology, yield, and climate variability and are increasingly being used in climate crop interaction studies[80,81]. In this study we train a random forest model on reported values of maize (soy) yield from 2003-2015 (1990-2015) for 36 (67) Brazilian microregions[82] using historical climate data from NOAA's Center for Weather and Climate Prediction dataset. Average yields vary substantially across our study region, due primarily to differences in agricultural management and climate. However, as we are interested in capturing the effect of climate on yield, and do not explicitly consider management, we eliminate microregions with long term average yield in the bottom 10%. We further require at least 10 years of yield data for a microregion to be included in the model. As a result of this, our final analysis consists of 36 (67) microregions, primarily in the Mato Grosso region in which average annual maize (soy) yields vary from 900 (2200) kg/ha to 6800 (3200) kg/ha.

The maize and soy models are both developed using the same eight predictor variables: (1) Year, (2) centroid latitude; (3) centroid longitude; (4) average growing season maximum temperature; (5) average growing season minimum temperature; (6) total growing season precipitation; (7) growing season warm nights – the total number of days with minimum temperatures greater than 24°C; and (8) hot days - the total number of days with maximum temperatures greater than 35 °C Previous studies have used a 40°C threshold for soy senescence[83–85]. However most regions in our domain have very few if any days above 40°C in the historical period, making that threshold impractical for an empirical analysis. Comparable to other published crop models[47], the trained model explains 49% and 55% of the interannual maize and soy yield variance respectively (SFigure 43). Accumulated local effect (ALE) plots show the sensitivity of the predicted yield to each individual predictor variable (SFigures 44,45,47,48). Further, we perform a simple sensitivity analysis by either increasing or decreasing the five historical climate predictor variables by 10% and rerunning the model. Increasing the historical climate by 10% (warmer and wetter) results in a 12% (4%) decrease in maize (soy) yield, and decreasing the historical climate (colder and drier) results in a 18% (3%) increase (decrease) in maize (soy) yield averaged over the entire domain of interest. We quantify the impact of climate change, as a result of the corresponding land-cover change scenario, by using the WRF simulation output to drive our trained crop models.

Acknowledgements:

This study was funded by the Neukom Institute for Computational Science at Dartmouth College, United States Department of Agriculture National Institute of Food and Agriculture (2015-68007-23133 and 2018-67003-27406), National Science Foundation (BCS 184018), and Nelson A. Rockefeller Center at Dartmouth College. We thank Research Computing at Dartmouth College for their assistance with compiling and running WRF.

Data availability

The crop cover dataset is available at https://doi.org/10.7910/DVN/ZFHCTI.

Code availability

NCAR's WRF model is freely available for download at http://www2.mmm.ucar.edu/wrf/users/downloads.html.
All modifications made to the WRF model code are detailed in the main text and supplementary information. And code to train and run the crop models can be found at: https://github.com/tpartrid/BrazilCropModel.

Author Contributions: SAS, JMW, and TFP conceived and designed the experiments. SAS performed the climate modelling experiments and TFP performed yield analyses. SAS, JMW, and TFP analyzed the data. SAS wrote the manuscripts with contributions from JMW and TFP.

Competing Interests: We declare no competing interests.

References

1. O'Connell, C. S. *et al.* Balancing tradeoffs: Reconciling multiple environmental goals when ecosystem services vary regionally. *Environ. Res. Lett.* **13**, 064008 (2018).
2. Klink, C. A. & Machado, R. B. Conservation of the Brazilian Cerrado. *Conserv. Biol.* **19**, 707–713 (2005).

3. Françoso, R. D. *et al.* Habitat loss and the effectiveness of protected areas in the Cerrado Biodiversity Hotspot. *Nat. Conserv.* **13**, 35–40 (2015).
4. Oliveira, P. T. S. *et al.* Trends in water balance components across the Brazilian Cerrado. *Water Resour. Res.* **50**, 7100–7114 (2014).
5. Spera, S. A., Galford, G. L., Coe, M. T., Macedo, M. N. & Mustard, J. F. Land-use change affects water recycling in Brazil's last agricultural frontier. *Glob. Change Biol.* **22**, 3405–3413 (2016).
6. Nóbrega, R. L. B. *et al.* Effects of conversion of native cerrado vegetation to pasture on soil hydro-physical properties, evapotranspiration and streamflow on the Amazonian agricultural frontier. *PLOS ONE* **12**, e0179414 (2017).
7. Bustamente, M. M. C., Corbeels, M., Scopel, E. & Roscoe, R. Soil carbon storage and sequestration potential in the cerrado region of Brazil. (2006).
8. Silvério, D. V. *et al.* Agricultural expansion dominates climate changes in southeastern Amazonia: the overlooked non-GHG forcing. *Environ. Res. Lett.* **10**, 104015 (2015).
9. Prevedello, J. A., Winck, G. R., Weber, M. M., Nichols, E. & Sinervo, B. Impacts of forestation and deforestation on local temperature across the globe. *PLOS ONE* **14**, e0213368 (2019).
10. Butt, N., Oliveira, P. A. de & Costa, M. H. Evidence that deforestation affects the onset of the rainy season in Rondonia, Brazil. *J. Geophys. Res. Atmospheres* **116**, (2011).
11. Wright, J. S. *et al.* Rainforest-initiated wet season onset over the southern Amazon. *Proc. Natl. Acad. Sci.* **114**, 8481–8486 (2017).

12. Leite-Filho, A. T., Pontes, V. Y. de S. & Costa, M. H. Effects of Deforestation on the Onset of the Rainy Season and the Duration of Dry Spells in Southern Amazonia. *J. Geophys. Res. Atmospheres* **124**, 5268–5281 (2019).

13. Leite-Filho, A. T., Costa, M. H. & Fu, R. The southern Amazon rainy season: The role of deforestation and its interactions with large-scale mechanisms. *Int. J. Climatol.* 1–14 (2019) doi:10.1002/joc.6335.

14. Riskin, S. H. *et al.* Solute and sediment export from Amazon forest and soybean headwater streams. *Ecol. Appl.* **27**, 193–207 (2017).

15. Dias, L. C. P., Macedo, M. N., Costa, M. H., Coe, M. T. & Neill, C. Effects of land cover change on evapotranspiration and streamflow of small catchments in the Upper Xingu River Basin, Central Brazil. *J. Hydrol. Reg. Stud.* **4**, 108–122 (2015).

16. Panday, P. K., Coe, M. T., Macedo, M. N., Lefebvre, P. & Castanho, A. D. de A. Deforestation offsets water balance changes due to climate variability in the Xingu River in eastern Amazonia. *J. Hydrol.* **523**, 822–829 (2015).

17. Aragão, L. E. O. C. *et al.* Interactions between rainfall, deforestation and fires during recent years in the Brazilian Amazonia. *Philos. Trans. R. Soc. B Biol. Sci.* **363**, 1779–1785 (2008).

18. Houghton, R. Tropical deforestation as a source of greenhouse gas emissions. in *Tropical Deforesation and Climate Change* (IPAM, 2005).

19. Karstensen, J., Peters, G. P. & Andrew, R. M. Attribution of CO2emissions from Brazilian deforestation to consumers between 1990 and 2010. *Environ. Res. Lett.* **8**, 024005 (2013).

20. Lima, L. S. *et al.* Feedbacks between deforestation, climate, and hydrology in the Southwestern Amazon: implications for the provision of ecosystem services. *Landsc. Ecol.* **29**, 261–274 (2014).
21. United States Department of Agriculture. World Agricultural Production. (2019).
22. United States Department of Agriculture Foreign Agricultural Service. Global Agricultural Information Network Report: Brazil Grain and Feed Annual, BR 1907. (2019).
23. Instituto Brasileiro de Geographia e Estatistica. 2017 Censo Agropecuario. Tabela 6764. (2017).
24. Lee, J.-E. *et al.* Reduction of tropical land region precipitation variability via transpiration. *Geophys. Res. Lett.* **39**, (2012).
25. Arima, E. Y., Walker, R. T., Perz, S. & Jr, C. S. Explaining the fragmentation in the Brazilian Amazonian forest. *J. Land Use Sci.* **11**, 257–277 (2016).
26. Knox, R., Bisht, G., Wang, J. & Bras, R. Precipitation Variability over the Forest-to-Nonforest Transition in Southwestern Amazonia. *J. Clim.* **24**, 2368–2377 (2010).
27. Khanna, J., Medvigy, D., Fueglistaler, S. & Walko, R. Regional dry-season climate changes due to three decades of Amazonian deforestation. *Nat. Clim. Change* **7**, 200–204 (2017).
28. Oliveira, L. J. C., Costa, M. H., Soares-Filho, B. S. & Coe, M. T. Large-scale expansion of agriculture in Amazonia may be a no-win scenario. *Environ. Res. Lett.* **8**, 024021 (2013).
29. Coe, M. *et al.* The Forests of the Amazon and Cerrado Moderate Regional Climate and Are the Key to the Future. *Trop. Conserv. Sci.* **10**, 1–6 (2017).
30. Lawrence, D. & Vandecar, K. Effects of tropical deforestation on climate and agriculture. *Nat. Clim. Change* **5**, 27–36 (2015).

31. Bagley, J. E., Desai, A. R., Harding, K. J., Snyder, P. K. & Foley, J. A. Drought and Deforestation: Has Land Cover Change Influenced Recent Precipitation Extremes in the Amazon? *J. Clim.* **27**, 345–361 (2013).

32. Costa, M. H. & Pires, G. F. Effects of Amazon and Central Brazil deforestation scenarios on the duration of the dry season in the arc of deforestation. *Int. J. Climatol.* **30**, 1970–1979 (2010).

33. Alves, L. M., Marengo, J. A., Fu, R. & Bombardi, R. J. Sensitivity of Amazon Regional Climate to Deforestation. *Am. J. Clim. Change* **6**, 75–98 (2017).

34. Le Page, Y. *et al.* Synergy between land use and climate change increases future fire risk in Amazon forests. *Earth Syst. Dyn. Online* **8**, (2017).

35. Wright, J. S., Fu, R. & Heymsfield, A. J. A statistical analysis of the influence of deep convection on water vapor variability in the tropical upper troposphere. *Atmospheric Chem. Phys.* **9**, 5847–5864 (2009).

36. Malhado, A. C. M., Pires, G. F. & Costa, M. H. Cerrado Conservation is Essential to Protect the Amazon Rainforest. *AMBIO* **39**, 580–584 (2010).

37. Sampaio, G. *et al.* Regional climate change over eastern Amazonia caused by pasture and soybean cropland expansion. *Geophys. Res. Lett.* **34**, (2007).

38. Spangler, K. R., Lynch, A. H. & Spera, S. A. Precipitation Drivers of Cropping Frequency in the Brazilian Cerrado: Evidence and Implications for Decision-Making. *Weather Clim. Soc.* **9**, 201–213 (2017).

39. Spera, S. A., Winter, J. M. & Chipman, J. W. Evaluation of Agricultural Land Cover Representations on Regional Climate Model Simulations in the Brazilian Cerrado. *J. Geophys. Res. Atmospheres* **123**, 5163–5176 (2018).

40. CONAB. Acompanhamento da safra brasileira de graos. *Cia. Nac. Abast.* **6**, 1–113 (2019).

41. Araújo, M. L. S. de *et al.* Spatiotemporal dynamics of soybean crop in the Matopiba region, Brazil (1990–2015). *Land Use Policy* **80**, 57–67 (2019).

42. Pires, G. F. & Costa, M. H. Deforestation causes different subregional effects on the Amazon bioclimatic equilibrium. *Geophys. Res. Lett.* **40**, 3618–3623 (2013).

43. Swann, A. L. S., Longo, M., Knox, R. G., Lee, E. & Moorcroft, P. R. Future deforestation in the Amazon and consequences for South American climate. *Agric. For. Meteorol.* **214–215**, 12–24 (2015).

44. Apley, D. W. & Zhu, J. Visualizing the Effects of Predictor Variables in Black Box Supervised Learning Models. *ArXiv161208468 Stat* (2016).

45. Lobell, D. B. & Burke, M. B. On the use of statistical models to predict crop yield responses to climate change. *Agric. For. Meteorol.* **150**, 1443–1452 (2010).

46. Partridge, T. F. *et al.* Mid-20th century warming hole boosts U.S. maize yields. *Environ. Res. Lett.* (2019) doi:10.1088/1748-9326/ab422b.

47. Lobell, D. B., Schlenker, W. & Costa-Roberts, J. Climate Trends and Global Crop Production Since 1980. *Science* **333**, 616–620 (2011).

48. Zhao, C. *et al.* Temperature increase reduces global yields of major crops in four independent estimates. *Proc. Natl. Acad. Sci.* **114**, 9326–9331 (2017).

49. Casado, L. & Londoño, E. Under Brazil's Far-Right Leader, Amazon Protections Slashed and Forests Fall. *New York Times* (2019).

50. Skamarock, C. *et al.* A Description of the Advanced Research WRF Version 3. (2008) doi:10.5065/D68S4MVH.

51. Niu, G.-Y. *et al.* The community Noah land surface model with multiparameterization options (Noah-MP): 1. Model description and evaluation with local-scale measurements. *J. Geophys. Res. Atmospheres* **116**, (2011).

52. Yang, Z.-L. *et al.* The community Noah land surface model with multiparameterization options (Noah-MP): 2. Evaluation over global river basins. *J. Geophys. Res. Atmospheres* **116**, (2011).

53. Dee, D. P. *et al.* The ERA-Interim reanalysis: configuration and performance of the data assimilation system. *Q. J. R. Meteorol. Soc.* **137**, 553–597 (2011).

54. Georgescu, M., Lobell, D. B., Field, C. B. & Mahalov, A. Simulated hydroclimatic impacts of projected Brazilian sugarcane expansion. *Geophys. Res. Lett.* **40**, 972–977 (2013).

55. Mu, Q., Zhao, M. & Running, S. W. Improvements to a MODIS global terrestrial evapotranspiration algorithm. *Remote Sens. Environ.* **115**, 1781–1800 (2011).

56. Pei, L. *et al.* WRF Model Sensitivity to Land Surface Model and Cumulus Parameterization under Short-Term Climate Extremes over the Southern Great Plains of the United States. *J. Clim.* **27**, 7703–7724 (2014).

57. Massey, J. D., Steenburgh, W. J., Knievel, J. C. & Cheng, W. Y. Y. Regional Soil Moisture Biases and Their Influence on WRF Model Temperature Forecasts over the Intermountain West. *Weather Forecast.* **31**, 197–216 (2015).

58. Cuntz, M. *et al.* The impact of standard and hard-coded parameters on the hydrologic fluxes in the Noah-MP land surface model. *J. Geophys. Res. Atmospheres* **121**, 10,676-10,700 (2016).
59. MapBiomas Project - Collection 3.1 of the Annual Land Use Land Cover Maps of Brazil.
60. INPE. PRODES—Projeto de Monitoramento do Desmatamento na Amazônia Brasileira por Satélite (Monitoring Deforestation in the Brazilian Amazon by Satelite Project). (2019).
61. LAPIG. SIAD-Cerrado—Monitoramento Sistemático dos Desmatamentos no Bioma Cerrado. (2019).
62. Spera, S. Agricultural Intensification Can Preserve the Brazilian Cerrado: Applying Lessons From Mato Grosso and Goiás to Brazil's Last Agricultural Frontier. *Trop. Conserv. Sci.* **10**, 1940082917720662 (2017).
63. Rausch, L. L. *et al.* Soy expansion in Brazil's Cerrado. *Conserv. Lett.* **12**, e12671 (2019).
64. Morton, D. C. *et al.* Reevaluating suitability estimates based on dynamics of cropland expansion in the Brazilian Amazon. *Glob. Environ. Change* **37**, 92–101 (2016).
65. Garrett, R. D. & Rausch, L. L. Green for gold: social and ecological tradeoffs influencing the sustainability of the Brazilian soy industry. *J. Peasant Stud.* **43**, 461–493 (2016).
66. Cohn, A. S. *et al.* Forest loss in Brazil increases maximum temperatures within 50 km. *Environ. Res. Lett.* **14**, 084047 (2019).
67. Sauer, S. Soy expansion into the agricultural frontiers of the Brazilian Amazon: The agribusiness economy and its social and environmental conflicts. *Land Use Policy* **79**, 326–338 (2018).
68. Jepson, W., Brannstrom, C. & Filippi, A. Access Regimes and Regional Land Change in the Brazilian Cerrado, 1972–2002. *Ann. Assoc. Am. Geogr.* **100**, 87–111 (2010).

69. Ho, J., Tumkaya, T., Aryal, S., Choi, H. & Claridge-Chang, A. Moving beyond P values: data analysis with estimation graphics. *Nat. Methods* **16**, 565–566 (2019).

70. 1. Companhia Nacional de Abastecimento. Calendário de Plantio e Colheita de Grãos no Brazil 2019. (2019).

71. Embrapa. Cultivo do Milho. in *Embrapa Milho e Sorgo* (2015).

72. Embrapa Soja. Tecnologias de produção de soja – Região Central do Brasil 2014. (2014).

73. Sibaldelli, R. N. R. & Farias, J. R. B. Boletim agrometeorológico da Embrapa Soja. *Embrapa Soja* (2016).

74. Schlenker, W. & Roberts, M. J. Nonlinear temperature effects indicate severe damages to U.S. crop yields under climate change. *Proc. Natl. Acad. Sci.* **106**, 15594–15598 (2009).

75. Ferreira, D. B. & Rao, V. B. Recent climate variability and its impacts on soybean yields in Southern Brazil. *Theor. Appl. Climatol.* **105**, 83–97 (2011).

76. Deryng, D., Sacks, W. J., Barford, C. C. & Ramankutty, N. Simulating the effects of climate and agricultural management practices on global crop yield. *Glob. Biogeochem. Cycles* **25**, (2011).

77. Viana, J. S., Gonçalves, E. P., Silva, A. C. & Matos, V. P. Climatic Conditions and Production of Soybean in Northeastern Brazil. *Compr. Surv. Int. Soybean Res. - Genet. Physiol. Agron. Nitrogen Relatsh.* (2013) doi:10.5772/52184.

78. Caratti, F. C., Lamego, F. P., Silva, J. D. G., Garcia, J. R. & Agostinetto, D. Partição da Competição por Recursos entre Soja e Milho Como Planta Competidora. *Planta Daninha* **34**, 657–666 (2016).

79. Breiman, L. Random Forests. *Mach. Learn.* **45**, 5–32 (2001).

80. Butler, E., Mueller, N. & Huybers, P. Peculiarly pleasant weather for US maize. *Proc. Natl. Acad. Sci.* **115**, 201808035 (2018).

81. Everingham, Y., Sexton, J., Skocaj, D. & Inman-Bamber, G. Accurate prediction of sugarcane yield using a random forest algorithm. *Agron. Sustain. Dev.* **36**, 27 (2016).

82. Instituto Brasileiro de Geographia e Estatistica. 2018 Producao Agricola Municpal. Tabela 839. (2019).

83. Deryng, D., Conway, D., Ramankutty, N., Price, J. & Warren, R. Global crop yield response to extreme heat stress under multiple climate change futures. *Environ. Res. Lett.* **9**, 034011 (2014).

84. Teixeira, E. I., Fischer, G., van Velthuizen, H., Walter, C. & Ewert, F. Global hot-spots of heat stress on agricultural crops due to climate change. *Agric. For. Meteorol.* **170**, 206–215 (2013).

85. Salem, M. A., Kakani, V. G., Koti, S. & Reddy, K. R. Pollen-Based Screening of Soybean Genotypes for High Temperatures. *Crop Sci.* **47**, 219–231 (2007).